Spray pyrolysis deposited multiferroic $BiFeO_3$ films

P. K. Siwach,[1] Jai Singh,[2] H. K. Singh,[1,a)] G. D. Varma,[3] and O. N. Srivastava[2]
[1]*National Physical Laboratory (CSIR), Dr. K. S. Krishnan Road, New Delhi 110012, India*
[2]*Department of Physics, Banaras Hindu University, Varanasi 221005, India*
[3]*Department of Physics, Indian Institute of Technology, Roorkee 247667, India*

(Presented 11 November 2008; received 1 October 2008; accepted 26 November 2008; published online 23 March 2009)

$BiFeO_3$ (BFO) films were prepared by nebulized spray pyrolysis technique on a single crystal $LaAlO_3$ (001) substrate at ~300 °C and annealing in oxygen at ~550 °C for 1 h. In all films BFO is the majority phase having a rhombohedrally distorted structure with $R3m$ symmetry and lattice parameters are $a=3.96$ Å and $\alpha=89.7°$. Atomic force microscopy reveals smooth and dense surface morphology. Despite the *G*-type antiferromagnetic spin structure of BFO the present BFO show well-defined *M-H* loops and unexpected ferromagnetism as evidenced by large saturation magnetization, ~125 emu/cc. The origin of anomalous ferromagnetism in the present films has been traced to the presence of nanometric Fe_2O_3 embedded in the BFO matrix. © *2009 American Institute of Physics*. [DOI: 10.1063/1.3072823]

I. INTRODUCTION

Multiferroics showing coexistence and synergistic coupling of polarization and magnetization in a single phase are both of fundamental interest, in elucidating just why they are so scarce, and of practical interest, for application in nonvolatile memory devices, spintronics, or actuators/transducers.[1–4] $BiFeO_3$ (BFO) is one of the very few promising natural multiferroic materials because of its above room temperature ferroelectric ($T_C \sim 1103$ K) and antiferromagnetic ($T_N \sim 643$ K) transitions.[5] It crystallizes in a rhombohedrally distorted perovskite structure with space group $R3c$ ($a=b=c=5.638$ Å, $\alpha=59.348°$).[5] Though BFO is promising there are still several issues: (1) difficulty in synthesizing single-phase samples, (2) weak polarization/ferromagnetism and low electrical resistivity at room temperature, and (3) variable oxidation states of Fe ions (Fe^{3+} to Fe^{2+}).[1] Wang *et al.*[5] reported enhanced remnant polarization ($P_r \sim 55$ C/cm^2) and saturation magnetization ($M_S \sim 80$ emu/cc) in (001) strained epitaxial BFO thin films that agrees nicely with theoretical calculations.[6] Thin films of BFO with the desired and reproducible multiferroic properties have been prepared by pulsed laser deposition, sputtering, sol gel, chemical solution deposition, and so on.[5,7–10] However, the multiferroic behavior varied remarkably in the samples and has been attributed to the synthesis techniques and processing parameters seem to play a decisive role on the multiferroic properties of BFO. In spray pyrolysis technique various synthesis parameters can be easily manipulated and it has many advantages, such as lower deposition temperature, precise control of composition, and better chemical homogeneity over large area.[11]

II. EXPERIMENTAL DETAILS

High purity iron nitrate and bismuth nitrate were used for the preparation of BFO (0.3*M*) precursor solution, which then sprayed on preheated $LaAlO_3$ (LAO/001) substrates maintained at ~(300 ± 5) °C. After the deposition, the films were annealed in flowing oxygen at ~550 °C for 1 h. More details are given elsewhere.[12] Phase analysis and crystallinity of the films were checked by x-ray diffraction (XRD) (X'Pert-Pro, Panalytical). The surface microstructure was examined by atomic force microscopy (AFM) (Nanoscope E) in contact mode. Microstructure characterization was done using transmission electron microscopy (TEM) (Tecnai-G^2 20, FEI) and energy dispersive x-ray analysis (EDAX) attached with TEM has been employed to study the overall cationic stoichiometry of the films. The magnetic properties [zero-field cooled (ZFC) and field cooled (FC) magnetizations] were measured by a vibrating sample magnetometer (PPMS, Quantum Design).

III. RESULTS AND DISCUSSION

In the XRD pattern (Fig. 1) of the BFO film all high intensity reflections were indexed with a rhombohedral dis-

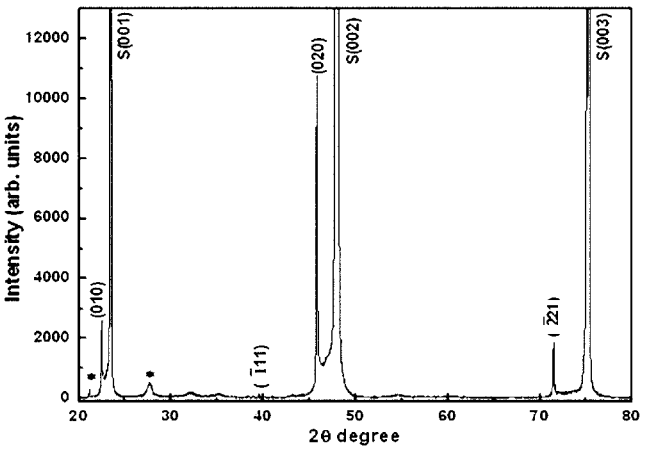

FIG. 1. XRD pattern of oxygenated BFO film showing dominantly single phasic rhombohedral distorted perovskite structure with traces of weak secondary phases.

a)Author to whom correspondence should be addressed. Electronic mail: hks65@mail.nplindia.ernet.in.

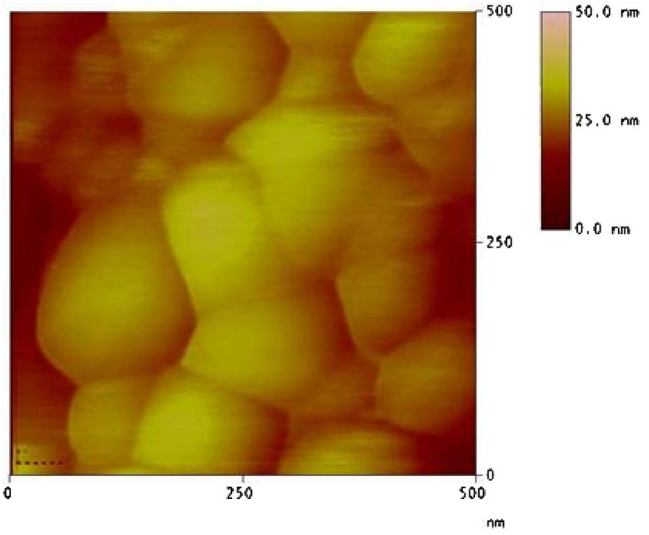

FIG. 2. (Color online) AFM surface morphology of oxygenated BFO film shows dense microstructure with uniform grains of ~250 nm.

torted perovskite structure (space group $R3m$),[13] with lattice parameters $a=3.96$ Å and $\alpha=89.7°$.[8,12] The films possess $(0k0)$ preferred orientation, as evident by the strongest (010) peak at 2θ angle of 22.44°. In addition to the BFO few weak reflections corresponding to Bi_2O_3 and Bi-rich secondary phases also appear. It has been observed that the deposition temperature and oxygen pressure have a significant effect on the evolution of various Fe- and Bi-rich phases in BFO thin films.[14–16] Bea *et al.*[15] found that a pure BFO phase is formed close to 10^{-2} mbar oxygen pressure and at 580 °C. Lower temperature or higher pressure is more conducive for Bi_2O_3 formation while at lower pressure or higher temperature yields γ-Fe_2O_3 phase. The diffraction pattern does not have any peak belonging to the Fe-rich phases such as α- or γ-Fe_2O_3 and Fe_3O_4. In the case of oriented growth, peaks of Fe_3O_4 or Fe_2O_3 phases are very close to BFO. Surface morphology as observed by AFM is quite dense and fairly smooth (Fig. 2) without any kind of outgrowth of Bi_2O_3 crystallites as observed by others.[10,14–16] In the present BFO film oxygenation and dense surface morphology suppress the formation of oxygen vacancies, i.e., valence fluctuations of Fe ions and grain boundary density, respectively. This results in high resistivity of the order of 10^{12} Ω cm, much better than that of other BFO films (10^9 Ω cm).[5]

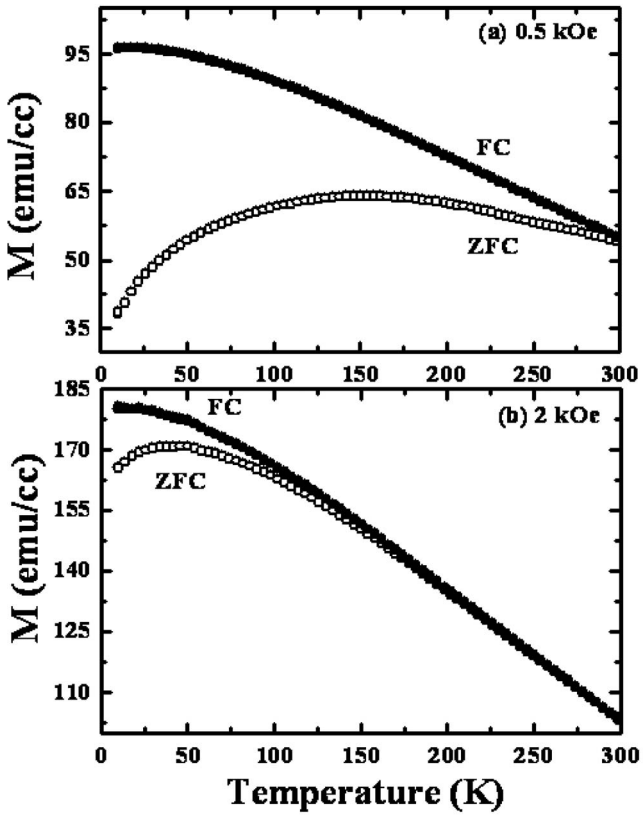

FIG. 3. Temperature dependence of magnetization of oxygenated BFO film at (a) 0.5 and (b) 2 kOe showing divergence in ZFC and FC magnetizations.

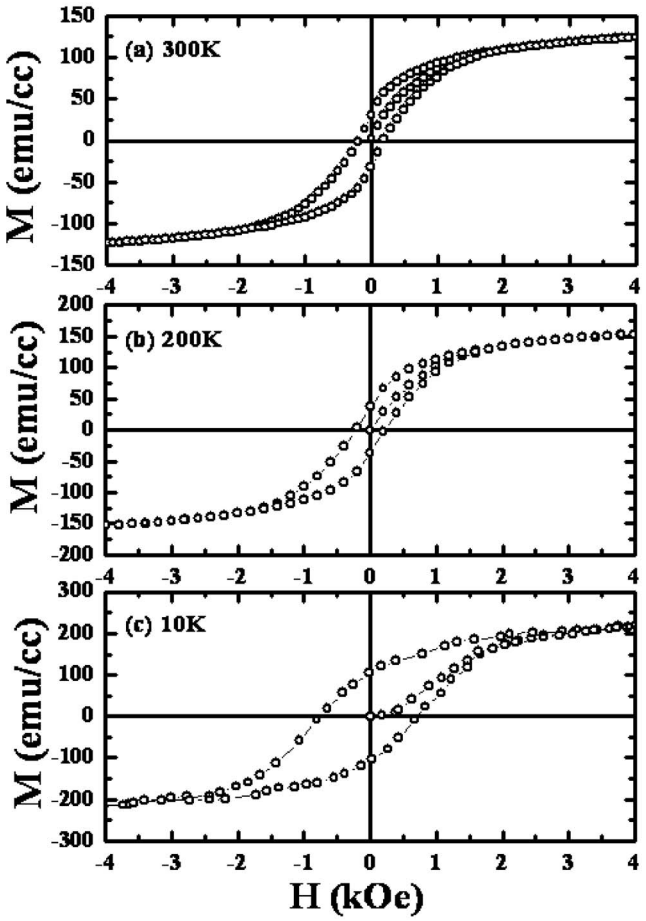

FIG. 4. *M-H* loop of oxygenated BFO film at different temperatures: (a) 300, (b) 200, and (c) 10 K.

The ZFC and FC magnetizations for BFO film measured at $H=0.5$ and 2 kOe are shown in Figs. 3(a) and 3(b), respectively. At $H=0.5$ kOe, ZFC curve shows a broad peak at ~156 K, which shifts toward significantly lower temperatures (~45 K) when the magnetic field is increased to 2 kOe. Strong divergence between the ZFC-FC curves beginning at $T\sim300$ K is observed at $H=0.5$ kOe and is significantly suppressed to ~150 K as the field is increased to 2 kOe. The observed ZFC-FC divergence have its origin in competing interaction among interacting magnetic clusters comprising of antiferromagnetic-BFO and

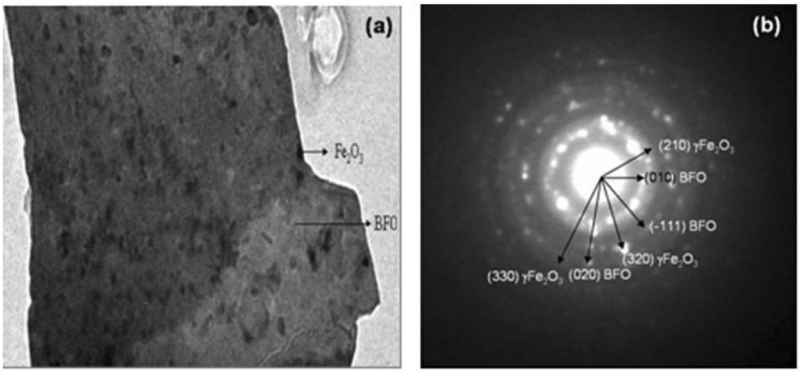

FIG. 5. (a) Transmission electron micrograph of BFO film embedded with Fe_2O_3 phases, and (b) SAD pattern of BFO and Fe_2O_3 phases.

ferromagnetic-Fe_2O_3. Figure 4 shows the typical S-shape magnetic hysteresis (M-H) loops measured at 300, 200, and 10 K. At 300 K the M_S (saturation magnetization), M_R (remnance), and H_C (coercivity) values are ~125 emu/cc, 30 emu/cc, and 190 Oe, respectively, which are higher than previously reported values.[5,7–9,14–16] At 10 K, M_S and M_R increase to ~230 and 100 emu/cc, respectively, while H_C ~370 Oe. As mentioned earlier, the present thicker BFO film having a $R3m$ structure is less rhombohedrally distorted than $R3c$,[8] and this suppresses the spatially modulated spin structure and hence causes weak ferromagnetism due to spin canting.[6,8–10] However, additional magnetization due to some kind of magnetic layer having ferromagnetic-Fe_2O_3 rich nanoclusters or precipitates can not be ruled out because γ-Fe_2O_3 have large magnetization of ~400 emu/cc.[14–16]

To search the microscopic magnetic clusters (e.g., Fe_2O_3) as the source of large anomalous magnetization we carried out TEM investigation [Figs. 5(a) and 5(b)]. The typical TEM microstructure of the film [Fig. 5(a)] consists of dark regions embedded in the brighter matrix. The EDAX spectrum from the bright and dark regions confirmed the presence of BFO and Fe_2O_3 phases, respectively. The corresponding selected area diffraction (SAD) patterns from the bright region could be indexed as the (010), ($\bar{1}$11), and (020) planes of BFO [Fig. 5(b)]. The lattice parameter for the present BFO film as evaluated by the SAD analysis of the (010) diffraction comes out to be a=3.95 Å. The indexing of this SAD pattern reveals the presence of BFO and Fe_2O_3 phases. It may be noticed that the diffuse rings in the pattern could be indexed as coming from (210), (320), and (330) planes of the γ-Fe_2O_3 phase. Thus TEM analysis confirms that the anomalous magnetism in these oxygenated BFO films is due to the presence of extrinsic ferromagnetic Fe_2O_3 phase embedded in the BFO matrix.

IV. CONCLUSION

High quality polycrystalline BFO films have been prepared on LAO (001) substrate by spray pyrolysis. XRD reveals dominantly single-phase oriented rhombohedral BFO films with traces of Bi-rich phases. AFM shows dense surface having a spherical grain size of ~250 nm. Oxygenation enhances crystallization and densification of BFO films. The saturation magnetization (M_S) increases from ~125 emu/cc at 300 K to ~230 emu/cc at 10 K. The observed anomalous ferromagnetism in BFO is due to the presence of γ-Fe_2O_3 clusters.

ACKNOWLEDGMENTS

Thanks are due to CSIR, New Delhi for funding and UGC-DAE CSR, Indore for research facilities. The authors are thankful to Professors V. Kumar and R. S. Tiwari for support and discussions.

[1] W. Prellier, M. P. Singh, and P. Murugavel, J. Phys.: Condens. Matter **17**, 7753 (2005).
[2] N. A. Hill, J. Phys. Chem. B **104**, 6694 (2000).
[3] W. Eerenstein, N. D. Mathur, and J. Scott, Nature (London) **44**, 759 (2004).
[4] R. Ramesh and N. A. Spaldin, Nature Mater. **6**, 21 (2007).
[5] J. Wang *et al.*, Science **299**, 1719 (2003).
[6] C. Ederer and N. A. Spaldin, Phys. Rev. B **71**, 060401 (2005).
[7] R. R. Das *et al.*, Appl. Phys. Lett. **88**, 242904 (2006).
[8] Y. Wang, Q. Jiang, H. He, and C. Nan, Appl. Phys. Lett. **88**, 142503 (2006).
[9] S. K. Singh, Y. K. Kim, H. Funakubo, and H. Ishiwara, Appl. Phys. Lett. **88**, 162904 (2006).
[10] J. Thery *et al.*, Chem. Vap. Deposition **13**, 232 (2007).
[11] P. K. Siwach *et al.*, J. Appl. Phys. **101**, 073912 (2007).
[12] P. K. Siwach, H. K. Singh, J. Singh, and O. N. Srivastava, Appl. Phys. Lett. **91**, 122503 (2007).
[13] JCPDS Card No. 72-2035.
[14] M. Murakami *et al.*, Appl. Phys. Lett. **88**, 112505 (2006).
[15] H. Bea *et al.*, Phys. Rev. B **74**, 020101 (2006).
[16] S. H. Lim *et al.*, Adv. Funct. Mater. **17**, 2594 (2007).